

Journal of
Cerebral Blood Flow
& Metabolism

**Glycolysis and pentose phosphate pathway after human
traumatic brain injury: microdialysis studies using 1,2-¹³C₂
glucose**

Journal:	<i>Journal of Cerebral Blood Flow and Metabolism</i>
Manuscript ID:	JCBFM-0300-14-ORIG.R1
Manuscript Type:	Original Article
Date Submitted by the Author:	16-Aug-2014
Complete List of Authors:	Jalloh, Ibrahim; University of Cambridge, Department of Clinical Neurosciences Carpenter, Keri; University of Cambridge, Neurosurgery; University of Cambridge, Wolfson Brain Imaging Centre Grice, Peter; University of Cambridge, Department of Chemistry Howe, Duncan; University of Cambridge, Department of Chemistry Mason, Andrew; University of Cambridge, Department of Chemistry Gallagher, Clare; University of Calgary, Department of Clinical Neurosciences Helmy, Adel; University of Cambridge, Neurosurgery Murphy, Michael; University of Cambridge, MRC Mitochondrial Biology Unit Menon, D; University of Cambridge, Division of Anaesthesia; University of Cambridge, Wolfson Brain Imaging Centre Carpenter, T Adrian; University of Cambridge, Wolfson Brain Imaging Centre Pickard, John; University of Cambridge, Neurosurgery; University of Cambridge, Wolfson Brain Imaging Centre Hutchinson, Peter; University of Cambridge, Neurosurgery; University of Cambridge, Wolfson Brain Imaging Centre
Keywords:	Brain trauma, Energy Metabolism, Glucose, Lactate, Neurochemistry

1
2
3 Title Page
4
5

6 **Glycolysis and pentose phosphate pathway after human traumatic brain injury:**
7 **microdialysis studies using 1,2-¹³C₂ glucose**
8
9

10
11 Ibrahim Jalloh MA¹, Keri L.H. Carpenter PhD^{1,2}, Peter Grice PhD³, Duncan J Howe BSc³,
12 Andrew Mason BSc³, Clare N. Gallagher MD PhD^{1,4}, Adel Helmy PhD¹, Michael P. Murphy
13 PhD⁵, David K. Menon PhD FRCP FMedSci^{2,6}, T. Adrian Carpenter PhD², John D. Pickard
14 PhD FRCS FMedSci^{1,2}, Peter J. Hutchinson PhD FRCS^{1,2}
15
16
17

18
19
20 *Authors' affiliations:*

21 ¹ Division of Neurosurgery, Department of Clinical Neurosciences, University of Cambridge,
22 UK;
23

24 ² Wolfson Brain Imaging Centre, Department of Clinical Neurosciences, University of
25 Cambridge, UK;
26

27 ³ Department of Chemistry, University of Cambridge, UK;
28

29 ⁴ Division of Neurosurgery, Department of Clinical Neurosciences, University of Calgary,
30 Canada;
31

32 ⁵ MRC Mitochondrial Biology Unit, Cambridge, UK;
33

34 ⁶ Division of Anaesthesia, Department of Medicine, University of Cambridge, UK
35
36

37
38 *Running title:* 1,2-¹³C₂ glucose metabolism in TBI
39
40

41 *Correspondence:*

42 Ibrahim Jalloh MA MRCS
43

44 University of Cambridge, Department of Clinical Neurosciences,
45

46 Division of Neurosurgery,
47

48 Box 167 Cambridge Biomedical Campus
49

50 Cambridge, CB2 0QQ
51

52 UK
53
54

55 Tel: +44 1223 596497; Fax: +44 1223 216926 Email: ij232@cam.ac.uk
56
57
58
59
60

Funding

We gratefully acknowledge financial support as follows. Study support: Medical Research Council (Grant Nos. G0600986 ID79068 and G1002277 ID98489) and National Institute for Health Research Biomedical Research Centre, Cambridge (Neuroscience Theme; Brain Injury and Repair Theme). Authors' support: I.J. – Medical Research Council (Grant no. G1002277 ID 98489) and National Institute for Health Research Biomedical Research Centre, Cambridge; K.L.H.C. – National Institute for Health Research Biomedical Research Centre, Cambridge (Neuroscience Theme; Brain Injury and Repair Theme); C.G. – the Canadian Institute of Health Research; A.H. – Medical Research Council/ Royal College of Surgeons of England Clinical Research Training Fellowship (Grant no. G0802251) and Raymond and Beverly Sackler Fellowship; D.K.M. and J.D.P. - National Institute for Health Research Senior Investigator Awards; P.J.H. – National Institute for Health Research Professorship, Academy of Medical Sciences/Health Foundation Senior Surgical Scientist Fellowship.

Disclosure/Conflict of Interest

J.D.P. and P.J.H. are Directors of Technicam.

Abstract

Increased 'anaerobic' glucose metabolism is observed after traumatic brain injury (TBI) attributed to increased glycolysis. An alternative route is the pentose phosphate pathway (PPP), which generates putatively protective and reparative molecules. To compare pathways we employed microdialysis to perfuse 1,2-¹³C₂ glucose into the brains of 15 TBI patients and macroscopically normal brain in 6 patients undergoing surgery for benign tumours, and to simultaneously collect products for NMR analysis. ¹³C enrichment for glycolytic 2,3-¹³C₂ lactate was median 5.4% (IQR 4.6-7.5%) in TBI brain and 4.2% (2.4-4.4%) in 'normal' brain (p<0.01). The ratio of PPP-derived 3-¹³C lactate to glycolytic 2,3-¹³C₂ lactate was median 4.9% (3.6-8.2%) in TBI brain and 6.7% (6.3-8.9%) in 'normal' brain. An inverse relationship was seen for PPP-glycolytic lactate ratio vs. P_{bt}O₂ (r=-0.5, p=0.04) in TBI brain. Thus, glycolytic lactate production was significantly greater in TBI than 'normal' brain. Several TBI patients exhibited PPP-lactate elevation above the 'normal' range. There was proportionally greater PPP-derived lactate production with decreasing P_{bt}O₂. The study raises questions about the roles of the PPP and glycolysis after TBI, and whether they can be manipulated to achieve a better outcome. This study is the first direct comparison of glycolysis and PPP in human brain.

Keywords: ¹³C-labelling, glycolysis, pentose phosphate pathway, lactate, traumatic brain injury (human)

Introduction

An increase in the proportion of glucose undergoing 'anaerobic' (non-oxygen consuming) metabolism is observed after traumatic brain injury (TBI).¹⁻³ This has been postulated to provide the energy in the form of adenosine triphosphate (ATP), produced via glycolysis, needed to restore ionic and neurochemical gradients, which become disturbed after TBI.^{4,5} Up-regulation of the pentose phosphate pathway (PPP) has also been suggested as a possible contributor to increased anaerobic glucose metabolism after TBI, based on rat models, and indirect (arteriovenous-jugular difference) studies in human patients.⁶⁻⁸

Glycolysis consists of the Embden-Meyerhof pathway from glucose to pyruvate, which does not use oxygen, and generates 2 moles of ATP per mole of glucose. Pyruvate can then be metabolised via the mitochondrial tricarboxylic acid cycle (TCA) cycle coupled to mitochondrial electron transport chains, which utilise oxygen in oxidative phosphorylation. The theoretical overall yield is 36 moles of ATP per mole of glucose. Alternatively, pyruvate can be converted to lactate, which recycles NADH (reduced nicotinamide-adenine dinucleotide) to NAD⁺, enabling further glucose molecules to be processed by glycolysis.

The PPP, also termed the hexose monophosphate shunt, is a biosynthetic pathway that constitutes a complex detour bypassing some of the steps of glycolysis in the metabolism of glucose. The key enzyme for the PPP, glucose-6-phosphate dehydrogenase, which is responsible for the rate-limiting step, is present in most tissues and cell types, and is regarded as a "housekeeping" enzyme.^{9,10} The PPP does not consume or produce ATP and does not require molecular oxygen. In the early "oxidative phase" of the PPP, during which the first carbon of the glucose skeleton is lost as carbon dioxide, nicotinamide adenine dinucleotide

1
2
3 phosphate (NADP⁺) is converted to NADPH. The latter is a reducing agent that participates
4
5 in reductive biosynthetic reactions, such as lipid and steroid synthesis, and in the production
6
7 of the reduced form of glutathione and thioredoxin. Glutathione and thioredoxin are cofactors
8
9 for glutathione peroxidase enzymes and peroxiredoxins respectively, both of which scavenge
10
11 hydroperoxides, thereby combatting oxidative stress. Among the many intermediates of the
12
13 later “non-oxidative” phase of the PPP is ribose 5-phosphate, used for nucleic acid synthesis.
14
15 Hence, the proportion of glucose metabolised via the PPP is greatest in tissues with high
16
17 lipid- and steroid-synthetic roles (e.g. liver and lactating mammary glands), also in cells with
18
19 a high oxidative load (e.g. red blood cells), and is thought to be one of the mechanisms
20
21 supporting high cell proliferation rates in cancer.¹⁰ PPP activity after TBI has been postulated
22
23 as playing a protective role, promoting synthesis of nucleic acids and fatty acids for tissue
24
25 repair and combatting the oxidative stress that results from injured cells.^{6,11}
26
27
28
29
30
31

32 Our aim was to evaluate glycolysis and the PPP as routes of glucose metabolism, directly in
33
34 TBI patients’ brains. Our novel approach was to perfuse the brain using a microdialysis
35
36 catheter with 1,2-¹³C₂ glucose and measure the ensuing labelling patterns in lactate collected
37
38 in the emerging microdialysates by analysing them using high-resolution nuclear magnetic
39
40 resonance (NMR) spectroscopy. For comparison, we also carried out the same technique in
41
42 ‘normal’ brain, and in muscle as a non-CNS tissue. The present study is the first direct
43
44 comparison of glucose metabolism via glycolysis and PPP in human brain.
45
46
47
48
49

50 **Materials and methods**

51 **Patients**

52
53
54 The Cambridge Central Local Research Ethics Committee approved this study. Informed
55
56 consent was obtained from all participants in the control ‘normal’ brain and muscle groups
57
58
59
60

1
2
3 and assent from the relatives of those patients who had suffered a TBI. The study was carried
4
5 out in conformation with the spirit and the letter of the Declaration of Helsinki.
6
7

8
9
10 *TBI brain microdialysis patients:* The TBI patients were defined as those suffering cranial
11
12 trauma with consistent CT scan findings and requiring invasive intracranial monitoring as
13
14 part of their clinical management. Patients were managed according to local TBI-
15
16 management protocols, which include endotracheal intubation, ventilation, sedation, and
17
18 muscular paralysis.¹²
19

20
21
22
23 *Control 'normal' brain microdialysis patients:* Patients undergoing a craniotomy for the
24
25 resection of a benign lesion whereby a microdialysis catheter could be safely placed into
26
27 radiographically normal brain were selected as control subjects. The microdialysis catheter
28
29 was placed via the craniotomy and tunnelled under the scalp. The control patients were
30
31 awake for the duration of microdialysis perfusion.
32
33

34
35
36 *Muscle microdialysis patients:* Patients undergoing resections of acoustic neuromas that
37
38 required thigh fat and fascia harvesting for dural closure were recruited for studying muscle,
39
40 for comparison with brain. During the procedure to harvest fat and fascia a microdialysis
41
42 catheter was placed under direct vision into quadriceps muscle. The muscle microdialysis
43
44 subjects were under general anaesthesia for the duration of the microdialysis perfusion, which
45
46 was performed at the same time of day for each patient minimising the effect of diurnal
47
48 variation.
49
50

51 52 53 54 **Microdialysis technique** 55 56 57 58 59 60

1
2
3 CMA 71 microdialysis catheters (membrane length 10 mm, nominal molecular weight cut-off
4 100 kDa) (M Dialysis AB, Stockholm, Sweden) were placed either via a triple lumen cranial
5 access device (Technicam, Newton Abbot, UK) or during a craniotomy for a traumatic
6 lesion, along with an intracranial pressure (ICP) monitor (Codman, Raynham, MA, USA) and
7 a Licox brain tissue oxygen sensor (GMS, Kiel-Mielkendorf, Germany) into frontal lobe. For
8 TBI patients with a diffuse injury, the right frontal region was chosen; if there was greater
9 injury to one hemisphere rather than the other, the most injured side was chosen. The catheter
10 was not placed within nor immediately adjacent to the lesion itself. CMA 71 catheters were
11 used for control 'normal' brain subjects and placed via the cranial opening at the end of their
12 neurosurgical procedure. CMA 60 catheters (membrane length 30 mm, nominal molecular
13 weight cut-off 20 kDa) were used for muscle subjects and placed under direct vision into
14 right quadriceps muscle following fat and fascia harvesting under general anaesthesia.
15
16
17
18
19
20
21
22
23
24
25
26
27
28
29
30
31

32 Catheters in the TBI patients and the normal brain control subjects were perfused with CNS
33 Perfusion Fluid (M Dialysis, AB), composed of NaCl (147 mmol/L), KCl (2.7 mmol/L),
34 CaCl₂ (1.2 mmol/L), and MgCl₂ (0.85 mmol/L) in water, supplemented with 4 mmol/L 1,2-
35 ¹³C₂ glucose (see below for details). Muscle microdialysis catheters were perfused with T1
36 Perfusion Fluid (M Dialysis AB), composed of NaCl (147 mmol/L), KCl (4 mmol/L), and
37 CaCl₂ (2.3 mmol/L) in water, supplemented with 4 mmol/L 1,2-¹³C₂ glucose. The
38 concentration (4 mmol/L) of ¹³C-labelled substrate was chosen to be within the range found
39 in brain and muscle microdialysates in unlabelled studies, to minimise perturbation.¹³⁻¹⁵ 1,2-
40 ¹³C₂ glucose (isotopic enrichment 99%, chemical purity 99%) was obtained from Cambridge
41 Isotope Laboratories, Inc (Tewksbury, MA) and was formulated in CNS perfusion fluid or T1
42 perfusion fluid by the Manufacturing Unit, Department of Pharmacy, Ipswich Hospital NHS
43 Trust (Ipswich, UK), who then tested the formulations to verify purity, sterility, freedom
44
45
46
47
48
49
50
51
52
53
54
55
56
57
58
59
60

1
2
3 from endotoxins and absence of pyrogenicity, to comply with current regulations, before
4 releasing them for use in patients. Microdialysate collection vials from the TBI patients were
5 changed hourly and analysed at the bedside using an ISCUS analyser (M Dialysis AB)
6 employing enzymatic colorimetric assays for glucose, lactate, pyruvate, glutamate and
7 glycerol. Microdialysate vials from 'normal' brain and from muscle were also analysed with
8 the ISCUS analyser at 4- and 2-hourly intervals, respectively. ICP, cerebral perfusion
9 pressure, and brain tissue oxygen tension ($P_{bt}O_2$) data from TBI patients were recorded at the
10 bedside using ICM+ software (ICM+, University of Cambridge, UK). Microdialysate
11 samples were stored at 4°C (or at -80°C if storage for longer than a few days was necessary)
12 prior to NMR analysis.
13
14
15
16
17
18
19
20
21
22
23
24
25
26

27 **NMR analysis**

28
29 Brain microdialysate samples were pooled into 24-hour periods for each individual patient.
30 For NMR analysis, 20 μ L of deuterium oxide (D_2O) and 50 μ L internal reference standard
31 from a stock solution of 24.0 mmol/L 3-(trimethylsilyl)-1-propanesulfonic acid sodium salt
32 (also termed 2,2-dimethyl-2-silapentane-5-sulfonate sodium salt or 4,4-dimethyl-4-
33 silapentane-1-sulfonate sodium salt; DSS) (Sigma-Aldrich, Poole, Dorset, UK) in CNS
34 perfusion fluid (M Dialysis) was added to 180 μ L of the pooled microdialysate sample.
35
36 Muscle microdialysate samples were pooled into 8-hour periods. 20 μ L of D_2O and 70 μ L
37 from a stock solution of 2.84 mmol/L DSS was added to 120 μ L of the pooled microdialysate
38 sample. Pooled samples, after addition of D_2O and DSS, were stored at -80°. For NMR
39 analysis, samples were transferred into 3 mm NMR tubes (Hilgenberg GmbH, Malsfeld,
40 Germany).
41
42
43
44
45
46
47
48
49
50
51
52
53
54
55
56
57
58
59
60

¹³C and ¹H NMR spectra were acquired on a Bruker Avance III HD 500 MHz spectrometer (Bruker BioSpin GmbH, Karlsruhe, Germany) with a dual ¹H/¹³C cryoprobe (CP DUL500C/H, Bruker BioSpin GmbH). ¹³C and ¹H NMR spectra were acquired and processed using TopSpin software (Bruker GmbH). ¹H spectra were acquired using the pulse programme noesypr1d, a 1D NOESY experiment using presaturation to suppress the water signal. Acquisition parameters included 32 scans with a d1 (relaxation delay) of 2s. ¹³C spectra were acquired using the pulse programme zgpg30, which has 30-degree flip-angle on the carbon channel, with a d1 of 3s, using 4096 (4k) scans and digitising 64K points. Power-gated broadband ¹H decoupling is achieved using the 'WALTZ-16' supercycle. The receiver gain is set to a constant value in each experiment. Metabolite signals in the samples were identified by comparison of their chemical shifts (ppm, reference DSS) to values from NMR databases (BMRB - Biological Magnetic Resonance Bank, University of Wisconsin¹⁶; HMDB - Human Metabolome Database, Genome Alberta¹⁷) and to those of our own standards. To confirm the identity of peaks, in selected cases, ¹H-¹³C heteronuclear single quantum correlation (HSQC) spectra were acquired on standards and patients' microdialysate samples.

To enable quantification of the signals in the ¹³C and ¹H 1-dimensional spectra, calibration was carried out with a series of known concentrations of standards including lactate, 3-¹³C lactate, glucose, 1,2-¹³C₂ glucose, and glutamine (from Sigma-Aldrich and Cambridge Isotope Laboratories). These standards were prepared in CNS Perfusion Fluid with the same fixed concentration of D₂O and DSS as for the preparation of brain microdialysate samples (see above) as an internal standard and run under identical NMR conditions to the pooled microdialysates. Peak areas for DSS, glucose, lactate and glutamine signals identified on the ¹³C and ¹H spectra were determined using combined Gaussian and Lorentzian line-shape

1
2
3 fitting. Peak areas relative to the DSS internal standard were used with reference to
4
5 calibration curves for each signal derived from standards (see above) of known
6
7 concentrations, which showed linear relationships between peak areas (ratio to DSS internal
8
9 standard) and concentrations. Fractional enrichment (%) is defined as $100 \times [^{13}\text{C}] / ([^{13}\text{C}] +$
10
11 $[^{12}\text{C}])$ where square brackets indicate concentrations of the relevant species. $[^{13}\text{C}]$ was
12
13 determined from the ^{13}C NMR spectra and $[^{12}\text{C}]$ from the ^1H spectra, using the calibration
14
15 method above. The natural abundance of ^{13}C is 1.1% of all carbon atoms, and ^{13}C results
16
17 presented for lactate (see Results section) were expressed after subtracting this natural
18
19 background from the ^{13}C singlet signals. ^{13}C doublet signals were not background-subtracted,
20
21 because the probability of two ^{13}C atoms occurring next to each other naturally is 0.01%.
22
23
24
25
26

27 Interpretation of the NMR results was based on biosynthetic pathways summarised
28
29 schematically in Fig. 1, which shows the lactate labelling patterns corresponding to
30
31 glycolysis, which produces 2,3- $^{13}\text{C}_2$ lactate, and the PPP, which produces 3- ^{13}C lactate.
32
33
34
35

36 **Statistical Analysis**

37
38 Statistical analyses performed using SPSS21 for Mac (IBM SPSS Statistics, NY) included
39
40 non-parametric tests (Mann-Whitney U-test and Kruskal–Wallis one-way analysis of
41
42 variance) with a preselected p-value of 0.05 for statistical significance. Results are presented
43
44 as median values with the interquartile range (IQR) given in parentheses. Relationships
45
46 between $P_{\text{bt}}\text{O}_2$ and the ^{13}C labelling results were explored using linear regression, with
47
48 Pearson's correlation coefficient r and analysis of variance (ANOVA) p values.
49
50
51
52
53

54 **Results**

55 **Demography**

56
57
58
59
60

1
2
3 Fifteen severe TBI patients (10 M, 5 F) aged 16-59 y (median 27 y) were studied using 1,2-
4 $^{13}\text{C}_2$ glucose (4 mmol/L) perfusion via the microdialysis catheter, with simultaneous
5 collection of microdialysates for NMR analysis. For comparison, macroscopically normal-
6 appearing brain was studied using the same ^{13}C -labelled microdialysis method in six patients
7 (age range 59-73 y; 3 M, 3 F) undergoing surgery for benign brain tumours. For a non-CNS
8 tissue comparison, thigh (quadriceps) muscle was similarly studied in four patients (age range
9 20-61 y; 3 M, 1 F) who underwent surgery for acoustic neuroma resection. A further seven
10 patients (2 'normal' brain, 5 muscle) were studied by microdialysis but with plain
11 unsupplemented perfusion fluid without 1,2- $^{13}\text{C}_2$ glucose. The 15 TBI patients who received
12 1,2- $^{13}\text{C}_2$ glucose (see above) were also studied for a baseline period with plain
13 unsupplemented perfusion fluid (without 1,2- $^{13}\text{C}_2$ glucose). Demographic details of all
14 patients are presented in Supplementary Table 1.
15
16
17
18
19
20
21
22
23
24
25
26
27
28
29
30
31

32 **Baseline results compared with 1,2- $^{13}\text{C}_2$ glucose perfusion period**

33
34 Microdialysate measurements (using the ISCUS analyser) of glucose, lactate, pyruvate,
35 glutamate and glycerol are shown in Fig. 2. These were acquired in the 15 TBI patients
36 during periods when the microdialysis catheter was perfused with plain unsupplemented CNS
37 perfusion fluid and also during the 24 h period of perfusion with 1,2- $^{13}\text{C}_2$ glucose (4
38 mmol/L). In 'normal' brain, ISCUS analysis was performed for two patients who received
39 plain unsupplemented perfusion fluid and for six patients who received 24 h perfusion with
40 1,2- $^{13}\text{C}_2$ glucose (4 mmol/L). In muscle, ISCUS analysis was performed for five patients who
41 received plain unsupplemented perfusion fluid, and for four patients who received 8 h
42 perfusion with 1,2- $^{13}\text{C}_2$ glucose (4 mmol/L). The 8 h period for muscle was necessitated due
43 to clinical practicalities of limb movement - microdialysis was limited to periods during the
44 acoustic neuroma surgery.
45
46
47
48
49
50
51
52
53
54
55
56
57
58
59
60

1
2
3
4
5
6
7
8
9
10
11
12
13
14
15
16
17
18
19
20
21
22
23
24
25
26
27
28
29
30
31
32
33
34
35
36
37
38
39
40
41
42
43
44
45
46
47
48
49
50
51
52
53
54
55
56
57
58
59
60

Significant increases ($p < 0.05$) in microdialysate glucose concentration (measured on the ISCUS analyser) between baseline (unsupplemented) and the 1,2- $^{13}\text{C}_2$ glucose perfusion period were seen for all three groups, as follows (medians): TBI brain (from 1.0 to 3.8 mmol/L), 'normal' brain (from 1.9 to 3.9 mmol/L) and muscle (from 2.8 to 5.3 mmol/L). The only other statistically significant, but not thought to be biologically significant, changes in ISCUS results between baseline and the 1,2- $^{13}\text{C}_2$ glucose perfusion period were for lactate/pyruvate ratio in TBI brain (from 22.2 to 24.8), for glycerol in TBI brain (from 52.0 to 69.6 $\mu\text{mol/L}$), and for glutamate in TBI brain (from 3.4 to 4.4 $\mu\text{mol/L}$) and muscle (from 7.9 to 29.7 $\mu\text{mol/L}$). Concentrations of 1,2- $^{13}\text{C}_2$ glucose (median and IQR) measured by ^{13}C NMR in the microdialysates from TBI brain (24 h perfusion period), normal brain (24 h perfusion period) and muscle (8 h perfusion period) were respectively 2.14 (1.45-2.43), 0.93 (0.83-1.83) and 0.95 (0.59-1.25) mmol/L, with TBI significantly different from normal brain ($p = 0.008$) or muscle ($p = 0.016$).

Throughout the 24 h period during which the cerebral microdialysis catheter was perfused with 1,2- $^{13}\text{C}_2$ glucose, the median serum glucose concentration measured in TBI patients was 7.3 mmol/L and all values were within the range 4-12 mmol/L except for one time-point in patient 11 where glucose was 1 mmol/L. Median serum lactate concentration was 1.1 mmol/L (min 0.7, max 3.0 mmol/L). (Supplementary Fig. 1).

NMR results for lactate production by glycolysis and PPP, and relationship with brain tissue oxygen

Illustrative examples of ^{13}C NMR spectra of the microdialysates are shown in Fig. 3. As a result of 1,2- $^{13}\text{C}_2$ glucose perfusion, TBI brain and 'normal' brain microdialysates included a

1
2
3 clearly visible doublet (red stars in expansion of ^{13}C spectra) for the lactate C3 methyl group,
4
5 and likewise a doublet for lactate C2, indicating glycolysis-derived 2,3- $^{13}\text{C}_2$ lactate, and a
6
7 smaller C3 singlet (green stars in expansion of ^{13}C spectra) representing PPP-derived 3- ^{13}C
8
9 lactate plus endogenous lactate. Qualitatively similar-appearing spectra were seen for muscle
10
11 microdialysates resulting from 1,2- $^{13}\text{C}_2$ glucose perfusion. Unlabelled TBI microdialysates
12
13 (with plain unsupplemented perfusion fluid) showed singlets for endogenous lactate C3 and
14
15 C2 (Fig. 3).
16
17
18
19

20
21 Natural abundance of ^{13}C was assumed 1.1%, and ^{13}C fractional enrichment values for lactate
22
23 were expressed after subtracting this naturally occurring ^{13}C background from the ^{13}C singlet
24
25 signals. In TBI brain microdialysates, ^{13}C fractional enrichment (%) in 2,3- $^{13}\text{C}_2$ lactate,
26
27 indicative of glycolysis, was median 5.4% (IQR 4.6-7.5%) measured using the C3 doublet
28
29 and this was significantly greater than in 'normal' brain (Fig. 4). Fractional enrichment was
30
31 based on quantification of the lactate C3 doublet signal (^{13}C spectrum) to measure ^{13}C at the
32
33 C3 position and the lactate methyl protons (attached to C3) triplet signal (^1H spectrum) to
34
35 quantify ^{12}C at the C3 position. Similar ^{13}C fractional enrichment to that of lactate C3 doublet
36
37 was obtained using the lactate C2 doublet, as expected (Fig. 4). In muscle, ^{13}C fractional
38
39 enrichment in 2,3- $^{13}\text{C}_2$ lactate was lower than in TBI and 'normal' brain (Fig. 4).
40
41
42
43
44

45 Based on the lactate C3 methyl group, ^{13}C fractional enrichment (%) in 3- ^{13}C lactate
46
47 indicative of the PPP in TBI brain microdialysates was median 0.24% (IQR 0.17-0.61%)
48
49 (Fig. 4) which was thus much less than the ^{13}C fractional enrichment in glycolytic 2,3- $^{13}\text{C}_2$
50
51 lactate (above). The ratio in TBI brain microdialysates of PPP-derived 3- ^{13}C lactate to
52
53 glycolytic 2,3- $^{13}\text{C}_2$ lactate was median 4.9% (IQR 3.6-8.2%) (Fig. 4). Four of the 15 TBI
54
55 patients exhibited ratios of PPP-derived to glycolytic lactate (11.4, 11.5, 11.9 and 14.0%) that
56
57
58
59
60

1
2
3 were greater than the range observed in the present study in normal brain (min 5.9, max
4
5 10.4%).
6

7
8
9 In muscle, microdialysis perfusion with 1,2-¹³C₂ glucose (4 mmol/L, for 8 h) resulted in
10 lactate C3 doublet and C2 doublet, indicating glycolytic 2,3-¹³C₂ lactate, with ¹³C enrichment
11 at C3 median 1.2% (range 1.0-1.4%). However, there was no ¹³C enrichment above
12 background natural abundance for lactate C3 singlet, so PPP production of lactate was not
13 detected in muscle.
14
15
16
17
18
19

20
21
22 The concentration of 2,3-¹³C₂ lactate (indicative of glycolysis) showed a non-significant
23 inverse trend ($r = -0.4$, $p = 0.1$) with brain tissue oxygen concentrations ($P_{bt}O_2$ expressed in
24 mm Hg) measured in the vicinity of the microdialysis catheter in TBI brain. A significant
25 inverse correlation ($r = -0.5$, $p = 0.04$) was seen for the ratio of PPP-lactate to glycolytic
26 lactate vs. $P_{bt}O_2$ (Fig. 5). Local tissue oxygen concentration was not measured in normal
27 brain or muscle.
28
29
30
31
32
33
34
35
36
37

38 Five TBI patients had a second 24 h period of 1,2-¹³C₂ glucose (4 mmol/L) microdialysis
39 perfusion. There were no significant differences in the production of glycolytic-lactate or
40 PPP-derived lactate between these two time periods.
41
42
43
44
45
46

47 Discussion

48 This study has shown that 1,2-¹³C₂ glucose infusion via the microdialysis catheter results in
49 ¹³C-labelling in lactate (Fig. 3) in the emerging microdialysates, enabling us to compare
50 glycolysis and PPP as routes by which lactate is derived. This is the first time this comparison
51 has been performed directly in human brain.
52
53
54
55
56
57
58
59
60

Glucose metabolism via glycolysis and the pentose phosphate pathway

Clear evidence for glycolysis being the main route of lactate production from glucose, as expected, was seen as diagnostic doublet signals for both C3 and C2 of lactate (Fig. 3) indicating 2,3-¹³C₂ lactate, a hallmark of the pathway (Fig. 1). These doublets were seen for all patients, in TBI brain, 'normal' brain and muscle. This is in accord with the recognised glycolysis pathway consisting of the Embden-Meyerhof pathway from glucose to pyruvate, followed by conversion to lactate by the action of lactate dehydrogenase (Fig. 1). This ¹³C enrichment was significantly higher in TBI brain, suggesting greater glycolytic activity, than in 'normal' brain and muscle. The doublet signals provide a distinctive signature that in effect avoids the issue of natural abundance ¹³C background (1% of all carbon atoms), since the probability of two endogenous ¹³C atoms occurring next to each other naturally is 0.01%.

The PPP loses the first carbon of 1,2-¹³C₂ glucose as carbon dioxide and thus gives rise to 3-¹³C lactate with a singlet signal for C3 (Fig 1). While ¹³C singlet signals for lactate C3 were clearly visible in all patients' microdialysates (Fig 3), these were smaller than the C3 doublet. Furthermore, it emerged that much of the C3 singlet signal intensity (peak area) was due to endogenous natural abundance ¹³C. Small ¹³C fractional enrichments for lactate C3 singlet above this background were seen in microdialysates from TBI brain and 'normal' brain, indicating PPP-derived lactate, but negligible in muscle. While there was no statistically significant difference in ¹³C fractional enrichment for lactate C3 between 'normal' brain and TBI brain, the higher upper range of the latter suggests that in certain TBI individuals lactate production via the PPP is elevated above that in 'normal' brain. In the four TBI patients with the most elevated PPP lactate, the ratio (%) of PPP lactate to glycolytic lactate was 11.4 – 14.0%.

1
2
3
4
5 Our finding of increased PPP activity in some patients as a result of brain injury is supported
6 by experimental studies. In rat models relevant to TBI, Bartnik et al. infused 1,2-¹³C₂ glucose
7 intravenously after fluid percussion injury and cortical contusion injury, and performed NMR
8 analysis of brain tissue extracts. They found an increase in the proportion of 3-¹³C lactate
9 (indicative of PPP) relative to 2,3-¹³C₂ lactate (indicative of glycolysis), in brain-injured rats
10 compared to control rats though with glycolysis remaining dominant.^{6,7} In humans, Dusick et
11 al. infused 1,2-¹³C₂ glucose intravenously, with ¹³C labelling in lactate assessed by
12 arteriovenous-jugular difference.⁸ This study in TBI patients and controls, although it did not
13 sample the brain directly and could only yield information on brain lactate labelling during
14 periods when the brain was a net exporter of lactate into the vasculature, led to similar
15 conclusions to the rat studies above.
16
17
18
19
20
21
22
23
24
25
26
27
28
29
30
31

32 **Significance of the PPP**

33
34 The PPP is a complex biosynthetic network generating many other species besides lactate
35 (Fig. 1) and the balance between these species can potentially shift depending on the local
36 biology and pathology. Some PPP-derived species are potentially reparative, e.g. ribose (for
37 nucleic acid synthesis) and NADPH (to provide reducing equivalents for fatty acid synthesis),
38 and neuroprotective e.g. NADPH, used for producing the reduced form of glutathione and
39 thioredoxin, which are cofactors for glutathione peroxidases and peroxiredoxins respectively,
40 enzymes that combat oxidative stress. Accordingly, Herrero-Mendez et al. (2009)
41 demonstrated that If one of the key regulatory enzymes of glycolysis, phosphofructokinase, is
42 activated in neurons so that more glucose is funnelled through glycolysis at the expense of
43 the PPP, apoptosis soon ensues due to oxidative stress.¹⁸ The PPP, which does not involve
44 molecular oxygen and does not generate ATP, can thus be regarded as sacrificing some of the
45
46
47
48
49
50
51
52
53
54
55
56
57
58
59
60

1
2
3 cells' supply of glucose molecules, which might otherwise have been used for ATP synthesis
4
5 via glycolysis and the TCA cycle, for the sake of generating more reducing power (NADPH)
6
7 and the ability to protect, repair or build cells.
8
9

10
11 NADPH is involved in many other biochemical reactions, e.g. NADPH is a cofactor for
12
13 NADPH oxidase and nitric oxide synthase and if these become dysregulated, oxidative stress
14
15 may ensue, with adverse consequences. Zuurbier et al. (2004) reported that inhibition of the
16
17 so-called "oxidative" phase of the PPP (the early steps of the PPP responsible for NADPH
18
19 production), by means of administering 6-aminonicotinamide, was cardioprotective in an
20
21 ischemia-reperfusion rat heart model.¹⁹ Interestingly, when Tyson et al. (2000) administered
22
23 6-aminonicotinamide to inhibit the PPP in rats in a study of brain using intravenous 2-¹³C
24
25 glucose as the substrate, they found that despite achieving PPP inhibition, evidenced by a
26
27 build-up of 6-phosphogluconate, there appeared to be a feedback effect of PPP inhibition on
28
29 glycolysis, such that both pathways decreased in a constant ratio.²⁰
30
31
32
33
34
35

36 **Role of brain tissue oxygen concentration in brain metabolism**

37
38 In the literature, 'hyperglycolysis' and the elevation of lactate production in the injured brain
39
40 have been attributed to hypoxia and/or mitochondrial dysfunction, though the exact nature of
41
42 the latter remains unclear. In a combined positron emission tomography (PET) (oxygen-15
43
44 and fluorodeoxyglucose (18F)) and microdialysis study, Vespa et al. (2005) reported that
45
46 'metabolic crisis' (defined as lactate/pyruvate ratio > 40) occurred in 7 out of 19 TBI patients
47
48 studied, though only one case showed regional ischaemia judged by PET.² In a microdialysis
49
50 study of 24 TBI patients in conjunction with $P_{bt}O_2$ measurement and perfusion CT, Sala et al.
51
52 (2013) concluded that the majority of lactate production was 'glycolytic' (rather than
53
54 hypoxic), albeit without evidence from carbon labelling.²¹
55
56
57
58
59
60

1
2
3
4
5 In the present study, we measured $P_{bt}O_2$ alongside the microdialysis catheter in the TBI
6 patients, and found that there was a non-significant trend towards greater glycolytically
7 generated 2,3- $^{13}C_2$ lactate with decreasing $P_{bt}O_2$. It is important to note that there were only 3
8 cases that could be described as hypoxic (defined as $P_{bt}O_2 < 20$ mm Hg), and the remaining
9 14 data-points ranged from 22 to 43 mm Hg. Interestingly, the ratio of PPP-derived lactate to
10 glycolytic lactate showed a significant inverse correlation with $P_{bt}O_2$ ($r = -0.5$, $p = 0.04$) (Fig
11 5). Thus, although PPP-derived lactate was always much less than glycolytic lactate, the
12 balance between the two appeared to shift towards the PPP with lower $P_{bt}O_2$. Like glycolysis,
13 the PPP does not utilise oxygen. Studies in adult rats and in brain slices have also suggested
14 that hypoxia increases the PPP.²² In contrast, Brekke et al. (2014) found evidence for a
15 decrease in PPP in neonatal rats after hypoxic-ischaemic injury, which the authors discussed
16 as paradoxical.²³ Moreover, they postulated that the apparent inability to up-regulate the PPP
17 in this situation might render the neonatal rats vulnerable. An analogous situation might
18 conceivably exist in human TBI, whereby low ability to up-regulate the PPP might result in
19 those individuals' brain tissue (either globally or locally) having increased risk of damage.
20
21 **Therapeutic up-regulation of the PPP in this context might be beneficial. Apart from**
22 **hypoxia (mentioned above), a few other up-regulators of the PPP have been identified.**
23 **Insulin has been shown to increase the expression of glucose-6-phosphate**
24 **dehydrogenase mRNA in primary rat hepatocytes.²⁴ Dehydroascorbate, the oxidised**
25 **form of vitamin C, has been shown to stimulate the activity of several PPP enzymes,**
26 **increase glutathione levels and inhibit hydrogen peroxide-induced changes in**
27 **mitochondrial transmembrane potential in Jurkat cells (a cancer cell line).²⁵ Although**
28 **these two latter studies were not performed in brain, they nevertheless illustrate the**
29
30
31
32
33
34
35
36
37
38
39
40
41
42
43
44
45
46
47
48
49
50
51
52
53
54
55
56
57
58
59
60

1
2
3 **principle that the PPP can be deliberately up-regulated with measurable biochemical**
4 **and biological effects.**
5
6

7 8 9 **Significance of lactate in the brain**

10 Lactate has been conventionally regarded as a waste product of glucose metabolism, though a
11 more recent idea is that it can act as a brain fuel - neurons take up lactate (produced from
12 glucose by glia), metabolise lactate to pyruvate, which is transported into the mitochondria
13 and converted to acetyl CoA, which enters the tricarboxylic acid (TCA) cycle. This has
14 become known as the astrocyte-neuron lactate shuttle hypothesis.²⁶ Animal studies have
15 provided evidence for brain utilisation of intravenously administered 3-¹³C lactate via the
16 TCA cycle.²⁷ In human brain, direct evidence for utilisation of lactate was first obtained in a
17 cerebral microdialysis study in TBI patients.²⁸ In the latter study, administration of 3-¹³C
18 lactate via the microdialysis catheter, and simultaneous collection of the emerging
19 microdialysates, with ¹³C NMR analysis, revealed ¹³C labelling in glutamine consistent with
20 lactate utilisation via the TCA cycle.²⁸ Recently, an intravenous lactate supplementation
21 study in TBI patients revealed evidence for a beneficial effect judged by surrogate
22 endpoints.²⁹ Studies of brain microdialysates (without supplementation) in 223 patients show
23 a statistical association between high extracellular lactate and unfavourable outcome.³⁰ Taken
24 together, available evidence suggests that where neurons are too damaged to utilise the
25 lactate produced from glucose by astrocytes, i.e. uncoupling of neuronal and glial
26 metabolism, high extracellular levels of lactate would accumulate, explaining one potential
27 mechanism behind the association between high extracellular lactate and poor outcome.
28
29
30
31
32
33
34
35
36
37
38
39
40
41
42
43
44
45
46
47
48
49
50
51

52 53 54 **Fate of lactate** 55 56 57 58 59 60

1
2
3 Regarding the possible fate of labelled lactate produced from 1,2-¹³C₂ glucose, a likely
4
5 scenario is that some of the labelled lactate is processed via the TCA cycle, and some of it
6
7 exported into the bloodstream. Since we were micro-dosing the brain with 1,2-¹³C₂ glucose
8
9 locally via the microdialysis catheter, it seemed highly unlikely that any of the ensuing
10
11 doubly labelled lactate would have been detectable in the bloodstream given the inevitable
12
13 dilution both with endogenous unlabelled lactate and with the volume of blood, so ¹³C NMR
14
15 analyses of blood were not performed.
16
17
18
19

20
21 Previously, using 3-¹³C lactate as the substrate, we detected singly labelled glutamine (and/or
22
23 glutamate) in TBI brain microdialysates, indicating utilisation of lactate via the TCA cycle.²⁸
24
25 In the present study, if 2,3-¹³C₂ lactate (produced from the substrate 1,2-¹³C₂ glucose) entered
26
27 the TCA cycle in brain cells, this would in theory have resulted in doublets in the ¹³C NMR
28
29 spectra, due to 4,5-¹³C₂ glutamine and 2,3-¹³C₂ glutamine (and/or glutamate in each case) on
30
31 the first turn of the cycle, and, on the second turn, doublets due to 1,2-¹³C₂ glutamine and a
32
33 singlet due to 3-¹³C glutamine.^{23,31} Experimental models of brain injury in rodents, using 1,2-
34
35 ¹³C₂ glucose as substrate, with analysis of brain tissue extracts representing total intracellular
36
37 and extracellular molecules, confirm double labelling in glutamate and glutamine.^{6,7,31} In our
38
39 present study, small singlet signals, but not doublets, corresponding to glutamine were seen
40
41 in the ¹³C NMR spectra of some of the microdialysates from 'normal' brain (4/6 patients) and
42
43 TBI (2/15 patients), verified by 2-D NMR methods, including ¹H-¹³C HSQC (Supplementary
44
45 Fig. 2). In theory, pyruvate cycling,³² which breaks the ¹³C-¹³C bond might explain the
46
47 glutamine singlets. Also, in theory, PPP-derived 3-¹³C lactate might enter the TCA cycle
48
49 forming singly-labelled glutamine (and/or glutamate), although accompanied by doubly-
50
51 labelled glutamine from glycolytic 2,3-¹³C₂ lactate, as found in vitro by Brekke et al.
52
53
54
55
56
57
58
59
60

1
2
3 (2012).³³ However, in the present study, quantification of the small glutamine singlets
4
5 revealed no significant ¹³C enrichment above natural abundance.
6
7

8
9
10 Microdialysis only samples the extracellular compartment and therefore cannot measure the
11
12 intracellular distribution of ¹³C. Even so, our ¹³C-labelled microdialysis method provides a
13
14 useful means for measuring 'early' glucose metabolism (glycolysis and PPP) as sufficient
15
16 labelled lactate is exported into the extracellular compartment to allow detection. However,
17
18 in the subsequent metabolism of lactate, the downstream dilution of ¹³C label with
19
20 endogenous unlabelled intermediates probably explains why we did not observe significant
21
22 ¹³C enrichment of extracellular metabolites derived from the TCA cycle. In our previous
23
24 study, when 3-¹³C lactate (4 mmol/L) or 2-¹³C acetate (4 mmol/L) was perfused via the
25
26 microdialysis catheter in TBI brain, labelling in glutamine consistent with TCA cycle was
27
28 seen in the emerging microdialysates.²⁸ However, in the same study, perfusion with 1-¹³C
29
30 glucose (2 mmol/L) resulted in negligible labelling in glutamine, consistent with the present
31
32 study.
33
34
35
36
37

38 **Strengths and limitations**

39
40 This ¹³C-labelled microdialysis method, performed in parallel with local brain tissue oxygen
41
42 measurement, provides a method of measuring glycolytic conversion of glucose into lactate
43
44 and at the same time distinguishing hypoxic from non-hypoxic glycolysis, as well as
45
46 evaluating the contribution of the PPP. Even though our evidence indicates a minor PPP-
47
48 derived lactate (3-¹³C lactate), it must be remembered that the PPP is a complex network of
49
50 biosynthetic reactions (Fig. 1) and it is conceivable that if heavy recycling is operating within
51
52 the PPP, less lactate might emerge, though with elevated production of NADPH and
53
54 intermediates utilised in neuroprotection and repair of cells.
55
56
57
58
59
60

1
2
3
4
5 The strategy of double labelling (using 1,2-¹³C₂ glucose as substrate) provides a characteristic
6
7 signature that appears in glycolytic lactate (2,3-¹³C₂ lactate) showing that the ¹³C-¹³C
8
9 covalent bond stays intact. Moreover the doublet signal is essentially free from endogenous
10
11 lactate as the probability of two ¹³C atoms being adjacent to each other naturally is 0.01%.
12
13 Like all cerebral microdialysis the ¹³C-labelled microdialysis method is invasive, so is only
14
15 suitable for severe TBI patients or those requiring brain surgery (e.g. for tumours), and it is a
16
17 focal technique.
18
19

20
21
22 This ¹³C-labelling method has the potential to be a useful adjunct to existing methodologies
23
24 of PET and unlabelled microdialysis in monitoring and studying TBI patients. The ¹³C-
25
26 labelled microdialysis method does not involve disruption of the patient's standard medical
27
28 care on the neurocritical care unit, and does not involve radioactivity or moving the patient to
29
30 a scanner. The 1,2-¹³C₂ glucose microdialysis method is reasonably inexpensive and
31
32 convenient to perform, since 1 or 2 g of the labelled material are enough to formulate enough
33
34 perfusion fluid for multiple patients, and the formulation can be stored in individual sterile
35
36 ready-to-use sealed glass vials in a refrigerator. The concentration (4 mmol/L) of 1,2-¹³C₂
37
38 glucose administered via microdialysis locally into brain corresponds to the upper end of the
39
40 'normal' range found in brain ECF.¹³ While conventional microdialysis performed with
41
42 unsupplemented perfusion fluid allows us to measure endogenous extracellular lactate, the
43
44 unsupplemented method cannot inherently distinguish between 'old' lactate and recently
45
46 synthesised lactate. An advantage of the 1,2-¹³C₂ glucose microdialysis method is that
47
48 enables measurement of labelled lactate production within a known timeframe – at present
49
50 this is 24h, because of current practical NMR considerations (see below).
51
52
53
54
55
56
57
58
59
60

1
2
3 A current limitation to our ^{13}C -labelled microdialysis method is the amount of material
4 necessary for performing NMR analysis. We have combined brain microdialysates for a 24h
5
6
7 period for each patient, to facilitate ^{13}C NMR spectroscopy within a convenient acquisition
8
9
10 time on the spectrometer. Our Bruker Avance 500 MHz spectrometer is equipped with a
11
12 cryoprobe, as used in the present study and in our previous study,²⁸ which is more sensitive
13
14 than non-cryo probe technology. Even so, the practical limit with our present equipment
15
16 limits us in terms of how short a timeframe we can analyse in terms of microdialysis
17
18 perfusion. Having better time-resolution for the microdialysis labelling results would be
19
20 useful from a biochemical perspective allowing time-course evaluation. $1,2\text{-}^{13}\text{C}_2$ glucose
21
22 microdialysis may have future potential for metabolic kinetic modelling of local glucose
23
24 consumption rates and glycolytic- and PPP- production rates of lactate. Commercially
25
26 available NMR micro-cryoprobes, which take smaller volumes, may be useful in future.
27
28 Analysis by mass spectrometry might also be useful in future, enabling smaller volumes to be
29
30 analysed, though at the expense of at least some of the detailed information on precise intra-
31
32 molecular position of label.
33
34
35
36
37

38 **Conclusion**

39
40 Here we have shown that ^{13}C labelled microdialysis can be used to interrogate glucose
41
42 metabolism via glycolysis and the PPP. The major pathway, glycolytic lactate production,
43
44 was significantly greater in TBI brain than in normal brain. The minor pathway, PPP-derived
45
46 lactate production, was statistically not significantly different in TBI brain than in normal
47
48 brain. However, several of the TBI individuals showed PPP-derived lactate elevation above
49
50 the range observed in normal brain. There was a shift in glucose metabolism from glycolysis
51
52 to PPP with decreasing brain tissue oxygen concentrations. The findings raise interesting
53
54 questions about the roles of the PPP and glycolysis after TBI, and whether they can be
55
56
57
58
59
60

1
2
3 manipulated to enhance the potentially reparative and antioxidant role of the PPP and
4
5 achieve a better outcome for the patient. The ^{13}C methodology developed here provides a
6
7 means of distinguishing recently synthesised lactate and its biosynthetic origin, and at the
8
9 same time measuring local oxygen tension alongside. ^{13}C -labelled microdialysis with 1,2-
10
11 $^{13}\text{C}_2$ glucose as substrate may thus find a methodological role in studies of hyperoxia or
12
13 strategies to optimise perfusion and mitochondrial function. This is the first time that a
14
15 comparison between glycolysis and the PPP has been carried out directly in human brain.
16
17
18
19

20 21 **Acknowledgments**

22
23 We thank Mr. R. Kirolos, Mr. R. Macfarlane and Mr. R. Mannion for assistance in placing
24
25 microdialysis catheters into the control subjects. We thank Dr. R.J. Shannon for assistance
26
27 with microdialysate analysis. We thank Mr. John Harwood (Ipswich Hospital NHS Trust) for
28
29 supervising the formulation of the ^{13}C substrate.
30
31
32
33

34 35 **Disclosure/Conflict of Interest**

36
37 J.D.P. and P.J.H. are Directors of Technicam.
38
39
40

41 42 **Supplementary Material**

43
44 Supplementary information is available at the Journal of Cerebral Blood Flow & Metabolism
45
46 website – www.nature.com/jcbfm
47
48
49
50
51
52
53
54
55
56
57
58
59
60

References

1. Bergsneider M, Hovda DA, Shalmon E, Kelly DF, Vespa PM, Martin NA, et al. Cerebral hyperglycolysis following severe traumatic brain injury in humans: a positron emission tomography study. *J Neurosurg* 1997;86:241–51.
2. Vespa P, Bergsneider M, Hattori N, Wu H-M, Huang S-C, Martin NA, et al. Metabolic crisis without brain ischemia is common after traumatic brain injury: a combined microdialysis and positron emission tomography study. *J Cereb Blood Flow Metab* 2005;25:763–74.
3. Wu H-M, Huang S-C, Vespa P, Hovda DA, Bergsneider M. Redefining the pericontusional penumbra following traumatic brain injury: evidence of deteriorating metabolic derangements based on positron emission tomography. *J Neurotrauma* 2013;30:352–60.
4. Katayama Y, Becker DP, Tamura T, Hovda DA. Massive increases in extracellular potassium and the indiscriminate release of glutamate following concussive brain injury. *J Neurosurg* 1990;73:889–900.
5. Kawamata T, Katayama Y, Hovda DA, Yoshino A, Becker DP. Administration of Excitatory Amino Acid Antagonists via Microdialysis Attenuates the Increase in Glucose Utilization Seen Following Concussive Brain Injury. *J Cereb Blood Flow Metab* 1992;12:12–24.
6. Bartnik BL, Sutton RL, Fukushima M, Harris NG, Hovda DA, Lee SM. Upregulation of pentose phosphate pathway and preservation of tricarboxylic acid cycle flux after experimental brain injury. *J Neurotrauma* 2005;22:1052–65.
7. Bartnik BL, Lee SM, Hovda DA, Sutton RL. The fate of glucose during the period of decreased metabolism after fluid percussion injury: a ¹³C NMR study. *J Neurotrauma* 2007;24:1079–92.
8. Dusick JR, Glenn TC, Lee WNP, Vespa PM, Kelly DF, Lee SM, et al. Increased pentose phosphate pathway flux after clinical traumatic brain injury: a [1,2-¹³C₂]glucose labeling study in humans. *J Cereb Blood Flow Metab* 2007;27:1593–602.
9. Pandolfi P, Sonati F, Rivi R, Mason P, Grosveld F, Luzzatto L. Targeted disruption of the housekeeping gene encoding glucose 6-phosphate dehydrogenase (G6PD): G6PD is dispensable for pentose synthesis but essential for defense against oxidative stress. *The EMBO Journal* 1995;14:5209.
10. Riganti C, Gazzano E, Polimeni M, Aldieri E, Ghigo D. The pentose phosphate pathway: An antioxidant defense and a crossroad in tumor cell fate. *Free Radical Biology and Medicine* 2012;53:421–36.
11. Ben-Yoseph O, Boxer PA, Ross BD. Assessment of the Role of the Glutathione and Pentose Phosphate Pathways in the Protection of Primary Cerebrocortical Cultures from Oxidative Stress. *J Neurochem* 1996;66:2329–37.

12. Helmy A, Vizcaychipi M, Gupta AK. Traumatic brain injury: intensive care management. *British Journal of Anaesthesia* 2007;99:32–42.
13. Reinstrup P, Ståhl N, Mellergård P, Uski T, Ungerstedt U, Nordström C. Intracerebral microdialysis in clinical practice: baseline values for chemical markers during wakefulness, anesthesia, and neurosurgery. *Neurosurgery* 2000;47:701–9–discussion709–10.
14. Rosdahl H, Ungerstedt U, Jorfeldt L. Interstitial glucose and lactate balance in human skeletal muscle and adipose tissue studied by microdialysis. *J Physiol* 1993;471:637–57.
15. Schulz MK, Wang LP, Tange M, Bjerre P. Cerebral microdialysis monitoring: determination of normal and ischemic cerebral metabolisms in patients with aneurysmal subarachnoid hemorrhage. *J Neurosurg* 2000;93:808–14.
16. Ulrich EL, Akutsu H, Doreleijers JF, Harano Y, Ioannidis YE, Lin J, et al. BioMagResBank [Internet]. *Nucleic Acids Res*2007 [cited 2013 Oct 11];36:D402–8. Available from: <http://www.bmrb.wisc.edu>
17. Wishart DS, Tzur D, Knox C, Eisner R, Guo AC, Young N, et al. HMDB: the Human Metabolome Database [Internet]. *Nucleic Acids Res*2007 [cited 2013 Oct 11];35:D521–6. Available from: <http://www.hmdb.ca>
18. Herrero-Mendez A, Almeida A, Fernández E, Maestre C, Moncada S, Bolaños JP. The bioenergetic and antioxidant status of neurons is controlled by continuous degradation of a key glycolytic enzyme by APC/C–Cdh1. *Nat Cell Biol* 2009;11:747–52.
19. Zuurbier CJ, Eerbeek O, Goedhart PT, Struys EA, Verhoeven NM, Jakobs C, et al. Inhibition of the pentose phosphate pathway decreases ischemia-reperfusion-induced creatine kinase release in the heart. *Cardiovasc Res* 2004;62:145–53.
20. Tyson RL, Perron J, Sutherland GR. 6-Aminonicotinamide inhibition of the pentose phosphate pathway in rat neocortex. *Neuroreport* 2000;11:1845–8.
21. Sala N, Suys T, Zerlauth J-B, Bouzat P, Messerer M, Bloch J, et al. Cerebral extracellular lactate increase is predominantly nonischemic in patients with severe traumatic brain injury. *J Cereb Blood Flow Metab* 2013;33:1815–22.
22. Domańska-Janik K. Hexose monophosphate pathway activity in normal and hypoxic rat brain. *Resuscitation* 1988;16:79–90.
23. Brekke EMF, Morken TS, Widerøe M, Håberg AK, Brubakk A-M, Sonnewald U. The pentose phosphate pathway and pyruvate carboxylation after neonatal hypoxic-ischemic brain injury. *J Cereb Blood Flow Metab* 2014;34:724–34.
24. Talukdar I, Szeszel-Fedorowicz W, Salati LM. Arachidonic acid inhibits the insulin induction of glucose-6-phosphate dehydrogenase via p38 MAP kinase. *J Biol Chem* 2005;280:40660–7.
25. Puskas F, Gergely P, Banki K, Perl A. Stimulation of the pentose phosphate pathway and glutathione levels by dehydroascorbate, the oxidized form of vitamin C. *FASEB J*

- 1
2
3 2000;14:1352–61.
4
5 26. Pellerin L, Magistretti PJ. Glutamate uptake into astrocytes stimulates aerobic
6 glycolysis: a mechanism coupling neuronal activity to glucose utilization. *Proc Natl*
7 *Acad Sci USA* 1994;91:10625–9.
8
9 27. Tyson RL, Gallagher CN, Sutherland GR. ¹³C-Labeled substrates and the cerebral
10 metabolic compartmentalization of acetate and lactate. *Brain Res* 2003;992:43–52.
11
12 28. Gallagher CN, Carpenter KLH, Grice P, Howe DJ, Mason A, Timofeev I, et al. The
13 human brain utilizes lactate via the tricarboxylic acid cycle: a ¹³C-labelled
14 microdialysis and high-resolution nuclear magnetic resonance study. *Brain*
15 2009;132:2839–49.
16
17 29. Bouzat P, Sala N, Suys T, Zerlauth J-B, Marques-Vidal P, Feihl F, et al. Cerebral
18 metabolic effects of exogenous lactate supplementation on the injured human brain.
19 *Intensive Care Med* 2014;40:412–21.
20
21 30. Timofeev I, Carpenter KLH, Nortje J, Al-Rawi PG, O'Connell MT, Czosnyka M, et al.
22 Cerebral extracellular chemistry and outcome following traumatic brain injury: a
23 microdialysis study of 223 patients. *Brain* 2011;134:484–94.
24
25 31. Bartnik BL, Hovda DA, Lee PWN. Glucose metabolism after traumatic brain injury:
26 estimation of pyruvate carboxylase and pyruvate dehydrogenase flux by mass
27 isotopomer analysis. *J Neurotrauma* 2007;24:181–94.
28
29 32. Cruz F, Cerdán S. Quantitative ¹³C NMR studies of metabolic compartmentation in
30 the adult mammalian brain. *NMR Biomed* 1999;12:451–62.
31
32 33. Brekke EMF, Walls AB, Schousboe A, Waagepetersen HS, Sonnewald U.
33 Quantitative importance of the pentose phosphate pathway determined by
34 incorporation of ¹³C from [2-¹³C]- and [3-¹³C]glucose into TCA cycle intermediates
35 and neurotransmitter amino acids in functionally intact neurons. *J Cereb Blood Flow*
36 *Metab* 2012;32:1788–99.
37
38 34. Carpenter KLH, Jalloh I, Gallagher CN, Grice P, Howe DJ, Mason A, et al. (¹³C)-
39 labelled microdialysis studies of cerebral metabolism in TBI patients. *Eur J Pharm Sci*
40 2014;57:87–97.
41
42
43
44
45
46
47
48
49
50
51
52
53
54
55
56
57
58
59
60

Titles and legends to figures

Fig. 1. Simplified schematic of steps in glycolysis and the pentose phosphate pathway (PPP), showing ^{13}C labelling patterns resulting from $1,2\text{-}^{13}\text{C}_2$ glucose substrate. Red fills indicate ^{13}C atoms. Abbreviations: Glc-6-P, glucose-6-phosphate; 6PGL, 6-phosphogluconolactone; F6P, fructose-6-phosphate; G3P, glyceraldehyde-3-phosphate; PYR, pyruvate. Figure originally published in *Eur J Pharm Sci* 2014; 57: 87-97 (Carpenter KLH et al.) under a Creative Commons Attribution License.³⁴

Fig. 2. ISCUS clinical microdialysis analyser measurements: at baseline (light grey bars) with plain unsupplemented perfusion fluid and during 24 h perfusion (brain: TBI or normal) or 8 h perfusion (muscle) with $1,2\text{-}^{13}\text{C}_2$ glucose (4 mmol/L) (dark grey bars). LPR is the lactate/pyruvate ratio. * $p < 0.05$ (Mann-Whitney) for baseline vs. perfusion with $1,2\text{-}^{13}\text{C}_2$ glucose. Box and whisker plots represent pooled data. Numbers of patients with baseline (unsupplemented) measurements were 15 TBI, 2 'normal' brain and 5 muscle. Numbers of patients who received $1,2\text{-}^{13}\text{C}_2$ glucose were 15 TBI, 6 'normal' brain and 4 muscle. 'Normal' brain was macroscopically normal-appearing brain in patients who underwent surgery for benign brain tumours. Muscle was leg quadriceps in patients undergoing acoustic neuroma resection surgery.

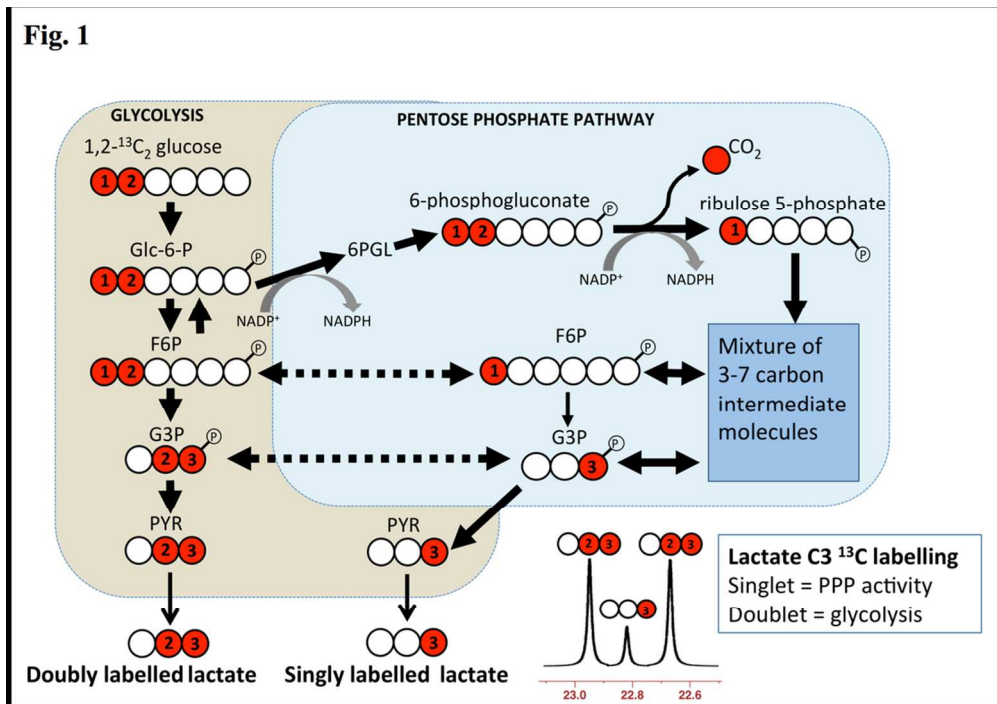
Fig. 3. Illustrative examples of ^{13}C NMR spectra for microdialysates from patients who received perfusion with $1,2\text{-}^{13}\text{C}_2$ glucose (4 mmol/L): TBI brain (uppermost two spectra, 24 h perfusion), 'normal' brain (third spectrum, 24 h perfusion), and muscle (bottom spectrum, 8 h perfusion). An example of brain microdialysate from an unlabelled TBI patient with plain (unsupplemented) perfusion fluid is shown for comparison (fourth spectrum). Examples of expansion of the lactate C3 signal are shown for TBI brain and 'normal' brain. Red stars

1
2
3 indicate lactate C3 doublet (due to glycolytic 2,3-¹³C₂ lactate) and green stars indicate C3
4
5 singlet (due to pentose phosphate pathway-derived 3-¹³C lactate plus endogenous lactate).
6

7 Abbreviations: glucose (Glc), lactate (Lac), 4,4-dimethyl-4-silapentane-1-sulfonate sodium
8 salt (DSS, the internal reference standard). Spectra were run from -20 ppm to +250 ppm. The
9
10 main reference DSS signal at 0 ppm is not shown in the range illustrated.
11
12
13

14
15
16 **Fig. 4.** Microdialysate NMR measurements of ¹³C labelling: results from perfusion for 24 h
17 (brain: TBI or 'normal') or 8 h perfusion (muscle) with 1,2-¹³C₂ glucose (4 mmol/L). Red
18 asterisks denote $p < 0.01$ for TBI vs. 'normal' brain (Mann-Whitney); other comparisons
19 asterisked in black denote $p < 0.05$. Individual data-points are shown by x symbols. Number
20 of patients: 15 TBI, 6 'normal' brain, 4 muscle.
21
22
23
24
25
26
27

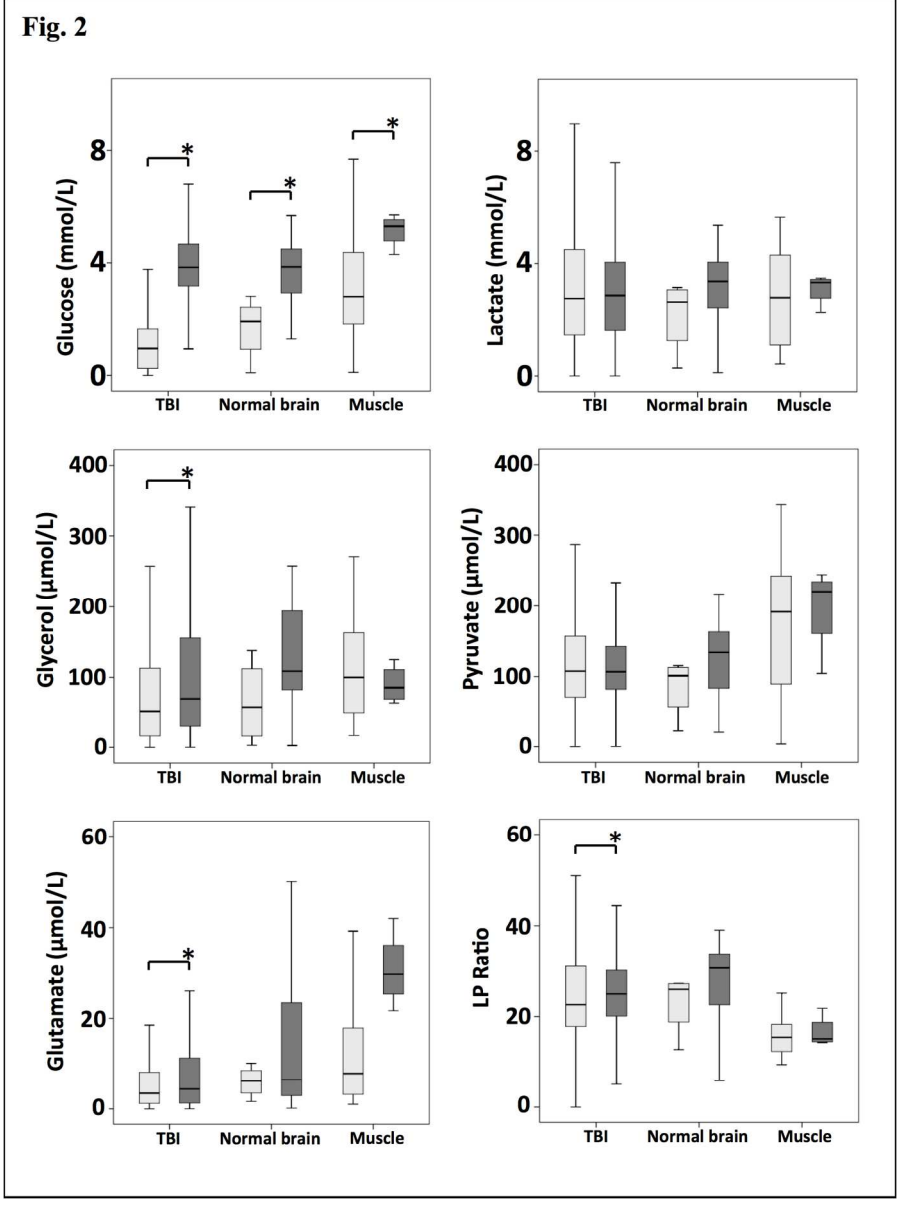
28
29
30 **Fig. 5.** Relationships in TBI brain for glycolytic lactate and pentose phosphate pathway
31 (PPP)-derived lactate vs. $P_{bt}O_2$. Concentrations of glycolytic 2,3-¹³C₂ lactate (upper panel)
32 and PPP-derived 3-¹³C lactate (middle panel) plotted vs. $P_{bt}O_2$. Lower panel: ratio (%) of
33 PPP-derived 3-¹³C lactate to glycolytic 2,3-¹³C₂ lactate, plotted vs. $P_{bt}O_2$. Each data-point
34 represents the results of NMR analysis of the combined contents of 24 x 1 h of
35 microdialysate collection vials from one microdialysis catheter, plotted against the
36 corresponding $P_{bt}O_2$ concentration expressed in mm Hg, measured using a Licox oxygen
37 probe placed alongside the microdialysis catheter in the brain. Lines are fitted by linear
38 regression (statistics shown are Pearson's correlation coefficient r and ANOVA p value).
39
40
41
42
43
44
45
46
47
48
49
50
51
52
53
54
55
56
57
58
59
60
61
62
63
64
65
66
67
68
69
70
71
72
73
74
75
76
77
78
79
80
81
82
83
84
85
86
87
88
89
90
91
92
93
94
95
96
97
98
99
100
101
102
103
104
105
106
107
108
109
110
111
112
113
114
115
116
117
118
119
120
121
122
123
124
125
126
127
128
129
130
131
132
133
134
135
136
137
138
139
140
141
142
143
144
145
146
147
148
149
150
151
152
153
154
155
156
157
158
159
160
161
162
163
164
165
166
167
168
169
170
171
172
173
174
175
176
177
178
179
180
181
182
183
184
185
186
187
188
189
190
191
192
193
194
195
196
197
198
199
200
201
202
203
204
205
206
207
208
209
210
211
212
213
214
215
216
217
218
219
220
221
222
223
224
225
226
227
228
229
230
231
232
233
234
235
236
237
238
239
240
241
242
243
244
245
246
247
248
249
250
251
252
253
254
255
256
257
258
259
260
261
262
263
264
265
266
267
268
269
270
271
272
273
274
275
276
277
278
279
280
281
282
283
284
285
286
287
288
289
290
291
292
293
294
295
296
297
298
299
300
301
302
303
304
305
306
307
308
309
310
311
312
313
314
315
316
317
318
319
320
321
322
323
324
325
326
327
328
329
330
331
332
333
334
335
336
337
338
339
340
341
342
343
344
345
346
347
348
349
350
351
352
353
354
355
356
357
358
359
360
361
362
363
364
365
366
367
368
369
370
371
372
373
374
375
376
377
378
379
380
381
382
383
384
385
386
387
388
389
390
391
392
393
394
395
396
397
398
399
400
401
402
403
404
405
406
407
408
409
410
411
412
413
414
415
416
417
418
419
420
421
422
423
424
425
426
427
428
429
430
431
432
433
434
435
436
437
438
439
440
441
442
443
444
445
446
447
448
449
450
451
452
453
454
455
456
457
458
459
460
461
462
463
464
465
466
467
468
469
470
471
472
473
474
475
476
477
478
479
480
481
482
483
484
485
486
487
488
489
490
491
492
493
494
495
496
497
498
499
500
501
502
503
504
505
506
507
508
509
510
511
512
513
514
515
516
517
518
519
520
521
522
523
524
525
526
527
528
529
530
531
532
533
534
535
536
537
538
539
540
541
542
543
544
545
546
547
548
549
550
551
552
553
554
555
556
557
558
559
560
561
562
563
564
565
566
567
568
569
570
571
572
573
574
575
576
577
578
579
580
581
582
583
584
585
586
587
588
589
590
591
592
593
594
595
596
597
598
599
600
601
602
603
604
605
606
607
608
609
610
611
612
613
614
615
616
617
618
619
620
621
622
623
624
625
626
627
628
629
630
631
632
633
634
635
636
637
638
639
640
641
642
643
644
645
646
647
648
649
650
651
652
653
654
655
656
657
658
659
660
661
662
663
664
665
666
667
668
669
670
671
672
673
674
675
676
677
678
679
680
681
682
683
684
685
686
687
688
689
690
691
692
693
694
695
696
697
698
699
700
701
702
703
704
705
706
707
708
709
710
711
712
713
714
715
716
717
718
719
720
721
722
723
724
725
726
727
728
729
730
731
732
733
734
735
736
737
738
739
740
741
742
743
744
745
746
747
748
749
750
751
752
753
754
755
756
757
758
759
760
761
762
763
764
765
766
767
768
769
770
771
772
773
774
775
776
777
778
779
780
781
782
783
784
785
786
787
788
789
790
791
792
793
794
795
796
797
798
799
800
801
802
803
804
805
806
807
808
809
810
811
812
813
814
815
816
817
818
819
820
821
822
823
824
825
826
827
828
829
830
831
832
833
834
835
836
837
838
839
840
841
842
843
844
845
846
847
848
849
850
851
852
853
854
855
856
857
858
859
860
861
862
863
864
865
866
867
868
869
870
871
872
873
874
875
876
877
878
879
880
881
882
883
884
885
886
887
888
889
890
891
892
893
894
895
896
897
898
899
900
901
902
903
904
905
906
907
908
909
910
911
912
913
914
915
916
917
918
919
920
921
922
923
924
925
926
927
928
929
930
931
932
933
934
935
936
937
938
939
940
941
942
943
944
945
946
947
948
949
950
951
952
953
954
955
956
957
958
959
960
961
962
963
964
965
966
967
968
969
970
971
972
973
974
975
976
977
978
979
980
981
982
983
984
985
986
987
988
989
990
991
992
993
994
995
996
997
998
999
1000



52x36mm (600 x 600 DPI)

Review Only

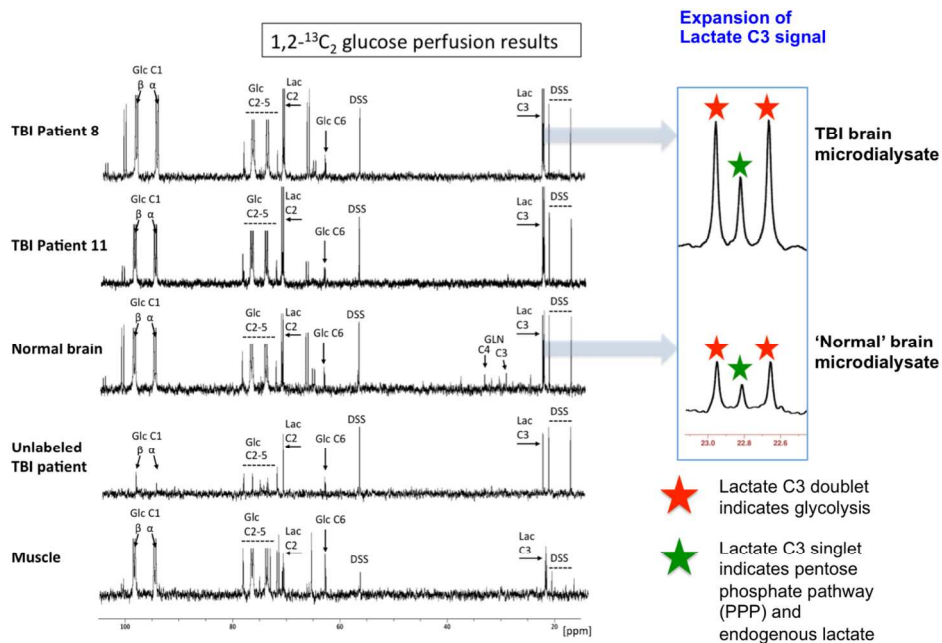
1
2
3
4
5
6
7
8
9
10
11
12
13
14
15
16
17
18
19
20
21
22
23
24
25
26
27
28
29
30
31
32
33
34
35
36
37
38
39
40
41
42
43
44
45
46
47
48
49
50
51
52
53
54
55
56
57
58
59
60



92x123mm (600 x 600 DPI)

only

Fig. 3

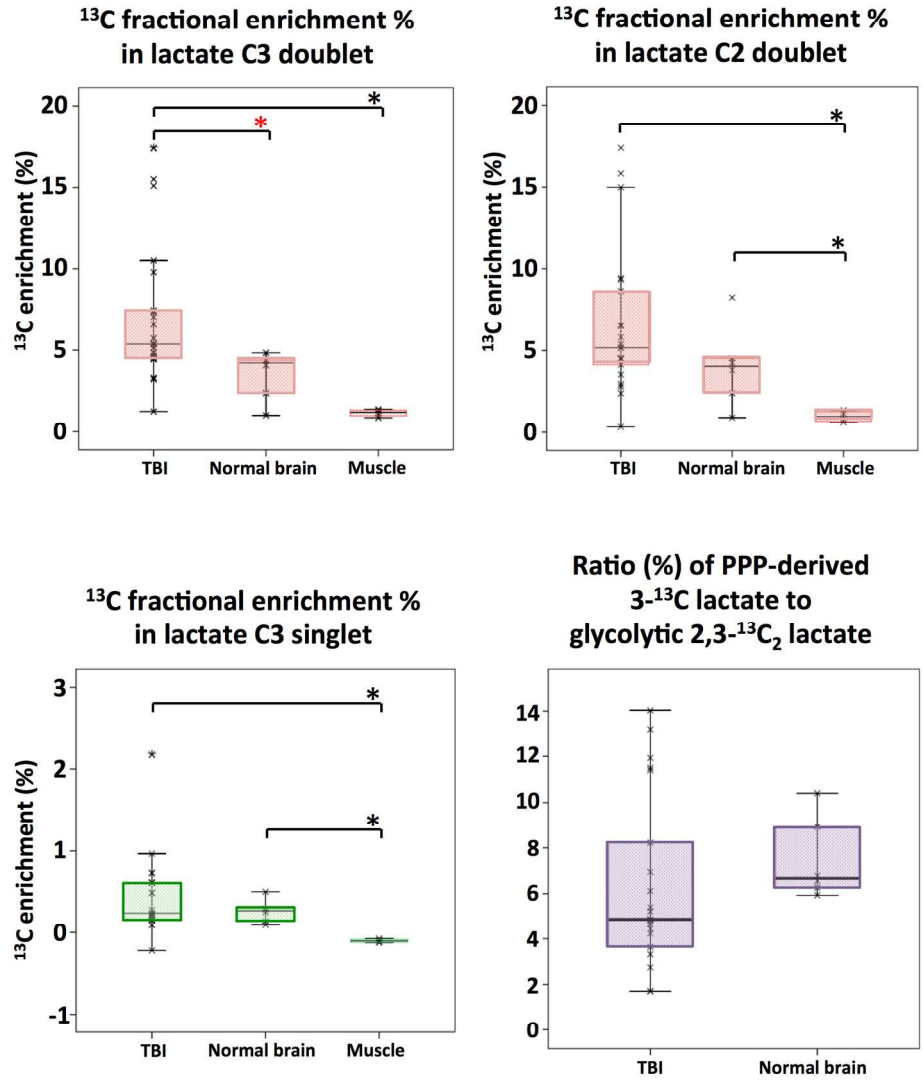


69x50mm (600 x 600 DPI)

Review Only

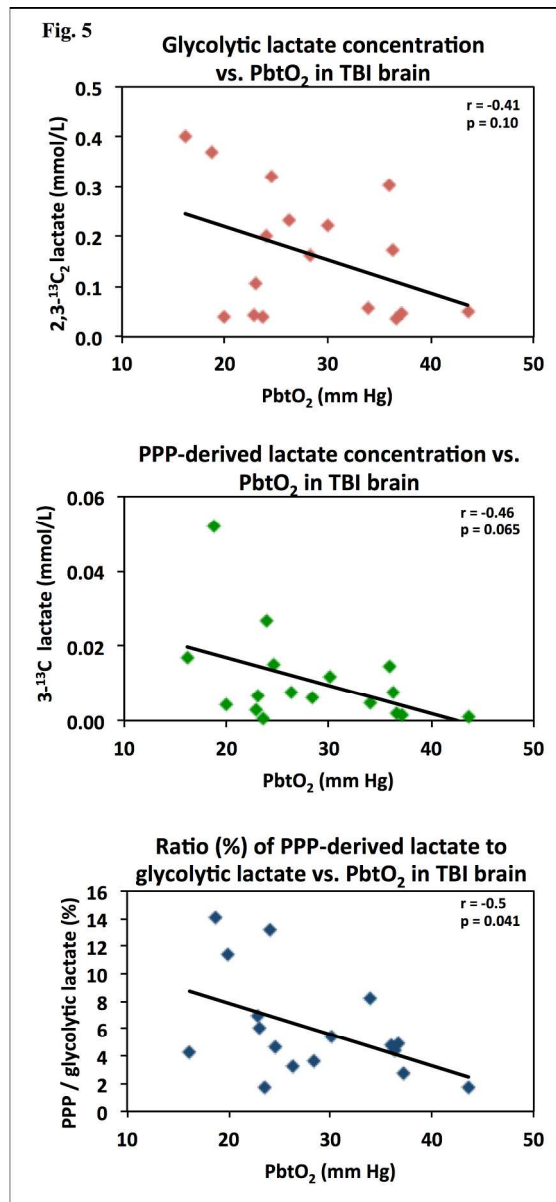
1
2
3
4
5
6
7
8
9
10
11
12
13
14
15
16
17
18
19
20
21
22
23
24
25
26
27
28
29
30
31
32
33
34
35
36
37
38
39
40
41
42
43
44
45
46
47
48
49
50
51
52
53
54
55
56
57
58
59
60

Fig. 4



86x104mm (600 x 600 DPI)

only



120x260mm (600 x 600 DPI)

only

1
2
3
4
5
6
7
8
9
10
11
12
13
14
15
16
17
18
19
20
21
22
23
24
25
26
27
28
29
30
31
32
33
34
35
36
37
38
39
40
41
42
43
44
45
46
47
48
49
50
51
52
53
54
55
56
57
58
59
60